TU Delft

Delft University of Technology

Document Version
Final published version

Citation (APA)
van den Brink, J. M., Scharff, H., Steinert, B., Melchior, S., Hrachowitz, M., Heimovaara, J., & Gebert, J. (2024). Long-term observations on the hydraulic performance of a combined capillary barrier-methane oxidation landfill cover system. *Waste Management*, *187*, 109-118. https://doi.org/10.1016/j.wasman.2024.07.002

Important note
To cite this publication, please use the final published version (if applicable).
Please check the document version above.

Copyright
In case the licence states “Dutch Copyright Act (Article 25fa)”, this publication was made available Green Open Access via the TU Delft Institutional Repository pursuant to Dutch Copyright Act (Article 25fa, the Taverne amendment). This provision does not affect copyright ownership.
Unless copyright is transferred by contract or statute, it remains with the copyright holder.

Sharing and reuse
Other than for strictly personal use, it is not permitted to download, forward or distribute the text or part of it, without the consent of the author(s) and/or copyright holder(s), unless the work is under an open content license such as Creative Commons.

Takedown policy
Please contact us and provide details if you believe this document breaches copyrights.
We will remove access to the work immediately and investigate your claim.

This work is downloaded from Delft University of Technology.

Green Open Access added to TU Delft Institutional Repository

'You share, we take care!' - Taverne project

https://www.openaccess.nl/en/you-share-we-take-care

Otherwise as indicated in the copyright section: the publisher is the copyright holder of this work and the author uses the Dutch legislation to make this work public.

Waste Management 187 (2024) 109–118

Contents lists available at ScienceDirect

Waste Management

journal homepage: www.elsevier.com/locate/wasman

Research Paper

Long-term observations on the hydraulic performance of a combined capillary barrier-methane oxidation landfill cover system

J.M. van den Brink [a,b], H. Scharff [c,d], B. Steinert [e], S. Melchior [e], M. Hrachowitz [f], T. J. Heimovaara [a], J. Gebert [a,*]

[a] Delft University of Technology, Department of Geoscience and Engineering, Stevinweg 1, 2628 CN Delft, the Netherlands
[b] Wageningen University & Research, Soil Physics and Land Management Group, Droevendaalsesteeg 3, 6708 PB Wageningen, the Netherlands
[c] N.V. Afvalzorg Holding, Nauerna 1, 1566 PB Assendelft, the Netherlands
[d] Landfill.pro, Den Haag, the Netherlands
[e] melchior + wittpohl Beratende Ingenieure PartmbB, Rödingsmarkt 43, 20459 Hamburg, Germany
[f] Delft University of Technology, Department of Water Management, Stevinweg 1, 2628 CN Delft, the Netherlands

ARTICLE INFO

Keywords:
Landfill cover
Capillary barrier system
Methane oxidation
Field test
Water balance
Diversion capacity
Hydraulic conductivity

ABSTRACT

This study quantifies the field hydraulic performance of a dual-functionality landfill cover, combining microbial methane oxidation with water diversion using a capillary barrier. The investigated 500 m^2 test field, constructed on a landfill in the Netherlands, consisted of a cover soil optimised for methane oxidation, underlain by a sandy capillary layer and a gravelly capillary block. Outflows from these layers were measured between 2009 and 2023. Average precipitation was 848 mm/a, evapotranspiration, diverted infiltration and breakthrough amounted to 504 (59.4 %), 282 (33.3 %) and 62 (7.3 %) mm/a, respectively. On average, the capillary barrier diverted 82 % of the inflow into the capillary layer. Breakthrough occurred mainly from October to March when evapotranspiration was low and the maximum water storage capacity of the cover soil was reached. During this period, inflow into the capillary barrier exceeded its diversion capacity, caused by the relatively high hydraulic conductivity of the cover soil due to its optimisation for gas transport. The diversion capacity declined drastically in the year after construction and increased again afterwards. This was attributed to suffusion of sand from the capillary layer into the capillary block and subsequent washout to greater depths or the influence of iron precipitates at the bottom of the capillary layer. The effect of a more finely grained methane oxidation layer on the hydraulic and methane oxidation performance should be investigated further. These measures could further improve the combined performance of the dual functionality landfill cover system under the given conditions of a temperate climate.

1. Introduction

Landfills pose a risk to human health and the environment due to the potential emissions of methane to the atmosphere and leachate potentially infiltrating the underlying soil and groundwater. Therefore the placement of an impermeable base liner in combination with a geological barrier and a landfill cover system comprising multiple functional layers, and the collection and treatment of gas and leachate are mandatory in many countries. One of the landfill cover designs that aims to limit both types of emissions simultaneously is a combination of a microbial methane oxidation system with a capillary barrier system. The latter limits the infiltration of precipitation from the cover soil into the waste body and hence reduces the amount of generated leachate.

The principle of microbial methane oxidation systems evolves around methanotrophic bacteria naturally present in a cover soil that oxidise methane to carbon dioxide. A so-called biocover, applied to cover a complete landfill or larger sections of it, can be cost-effective on landfills where emissions are relatively low or active gas extraction and treatment is no longer economically or technically viable (see reviews by Gebert et al., 2022; Huber-Humer et al., 2008; Scheutz et al., 2009). Such a system consists of at least two layers: a gas distribution layer with a methane oxidation layer (MOL) on top. A gas distribution layer evenly

* Corresponding author.
E-mail addresses: mark.vandenbrink@wur.nl (J.M. van den Brink), h.scharff@afvalzorg.nl (H. Scharff), steinert@mplusw.de (B. Steinert), melchior@mplusw.de (S. Melchior), m.hrachowitz@tudelft.nl (M. Hrachowitz), t.j.heimovaara@tudelft.nl (T.J. Heimovaara), j.gebert@tudelft.nl (J. Gebert).

https://doi.org/10.1016/j.wasman.2024.07.002
Received 31 January 2024; Received in revised form 8 June 2024; Accepted 2 July 2024
Available online 13 July 2024
0956-053X/© 2024 Published by Elsevier Ltd.

distributes landfill gas, which leaves the waste through hotspots, to the overlying methane oxidation layer, where the methane is oxidised using atmospheric oxygen.

A capillary barrier system is commonly used as part of a sloped landfill cover to limit infiltration of water into the waste body (e.g. Aubertin et al., 2009; Melchior, 1993; Rahardjo et al., 2016). It consists of a top layer of finer-grained mineral material, for example, sand (capillary layer, CL), overlying a layer of coarser mineral material, for example, gravel (capillary block, CB). Due to its finer average grain and, consequently, smaller pore sizes, the capillary layer has a higher moisture retention capacity than the capillary block. In addition, the capillary block is generally rather dry and hence has a very low hydraulic conductivity and behaves like a hydraulic barrier. Consequently, most of the precipitation that infiltrates into the capillary layer from the overlying cover soil is diverted downslope within the capillary layer and does not enter the capillary block (Fig. 1). However, when the matric potential in the capillary layer reaches the water entry value of the capillary block, water will start infiltrating into the capillary block, which is defined as breakthrough (Baker & Hillel, 1990; Stormont & Anderson, 1999). This condition depends on the infiltration rate into and the diversion capacity of the capillary layer, combined with the slope length (Oldenburg & Pruess, 1993; Ross, 1990; Yeh et al., 1994). The infiltration rate is controlled by the hydraulic conductivity and available water storage in the cover soil, which both depend on the cover soils' properties and the local climatic conditions. The diversion capacity is impacted by the slope angle and the (difference in) hydraulic properties of the capillary layer and capillary block (Aubertin et al., 2009; Kämpf et al., 2003; Khire et al., 2000; Ross, 1990; Steinert, 1999).

Capillary barriers generally perform well in (semi-) arid regions where potential evapotranspiration exceeds precipitation considerably (Khire et al., 1999; Stormont, 1996). In regions where precipitation exceeds potential evaporation during some part of the year, breakthrough is more likely to occur, as shown by various field studies investigating different capillary barrier system designs (Abdolahzadeh et al., 2011; Giurgea et al., 2003; Kämpf & Montenegro, 1997; Li et al., 2022). During such periods, excess precipitation either needs to be stored in the soil covering the capillary barrier system or within the capillary layer itself, or drained laterally to a point where the water can be collected (Khire et al., 2000; Li et al., 2022; Scarfone et al., 2023; Stormont & Morris, 1998; Yang et al., 2004).

Recent field studies used capillary barriers to prevent landfill gas from leaving or oxygen from entering a landfill (Ng et al., 2021; Zhan et al., 2020a) or a sulfidic mine waste tailing (Zhang et al., 2024). In contrast, several other studies have investigated the feasibility of combining the microbial methane oxidation function with the water diversion function of a capillary barrier in a landfill cover (Fig. 1). This design could be used in combination with or after active in situ treatment of landfilled wastes (Brand et al., 2016). In such a setup, the capillary block also serves as a gas distribution layer as it is mostly dry and highly permeable for gas flow. This landfill cover design has been studied in the laboratory (Berger et al., 2005; Wawra & Holfelder, 2003) as well as in the field (Geck et al., 2016; Röwer et al., 2016a, 2016b, Zhan et al., 2020b). Röwer et al., (2016a) and Geck et al. (2016) observed a satisfactory average oxidation efficiency of 77 % and 84 % respectively at a large-scale test field in the Netherlands. However, the oxidation showed a seasonal pattern with lower efficiencies in winter and higher efficiencies in summer. This was partly attributed to the accumulation of water at the bottom of the capillary layer in the periods of low evapotanspiration, due to the capillary barrier effect, especially in the downslope areas. It reduced the gas permeability, causing the landfill gas to migrate upslope, resulting in a higher local methane load to the cover and a lower oxidation efficiency (Ahoughalandari & Cabral, 2017; Wawra & Holfelder, 2003).

This study adds the aspect of the hydraulic performance of such a combined methane oxidation-capillary barrier system by analysing the water balance of the same test field as studied by Röwer et al., (2016a) and Geck et al. (2016) for the period between 2009 and 2023 (Fig. 1). Field observations of such a long duration for a capillary barrier system are rare, enabling analysis of the temporal variability of capillary barrier performance and its response to changing hydrological conditions.

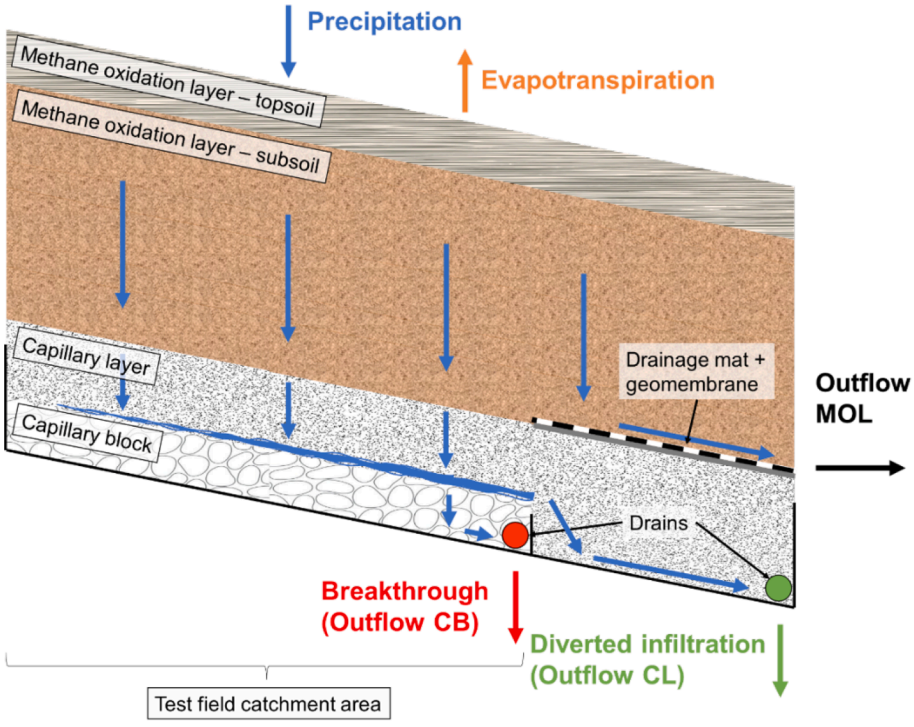


Fig. 1. Conceptual cross section of the test field in the downslope direction (not to scale) showing the landfill cover design with the incoming and outgoing water flows (MOL: methane oxidation layer, CL: capillary layer, CB: capillary block).

2. Materials and methods

2.1. Test field

2.1.1. Setup and construction

The test field of 500 m^2 horizontal surface area was constructed on a 1:5 slope in August 2009 on the landfill Wieringermeer, located in the northwest of the Netherlands (Fig. 2), comprising four soil layers: a methane oxidation layer topsoil and subsoil on top of the sandy capillary layer and the capillary block constructed from gravel (from top to bottom; Fig. 1). Grass was used as vegetation cover. Around the test field perimeter, vertical high-density polyethylene (HDPE) walls of 40 cm height were placed to prevent the inflow of external water and uncontrolled outflow of water from within the test field area. Above the collection zone of the diverted infiltration at the bottom end of the test field, a geomembrane was placed in order to prevent vertical seepage of water from the cover soil into the capillary layer. Above the geomembrane a drainage mat was installed to drain the seepage from the cover soil laterally. A boundary zone of 3 m width of identical soil layering was placed around the test field to negate any influences of the surrounding cover soil, which differs in soil properties and layering. The field and boundary area were underlain with a HDPE membrane to separate the test field from the waste body and enable the collection and quantification of percolating water. The soil was placed loosely with a long-range excavator to avoid a decrease in air capacity of the methane oxidation layer. Photos of the construction of the test field are presented in the Supplementary Material section S.1. After concluding that this air capacity was too high for optimal gas distribution, the top 60 cm of the methane oxidation layer was compacted in August 2013 using a bulldozer, which resulted in a more uniform gas distribution over the test field (Geck et al., 2016).

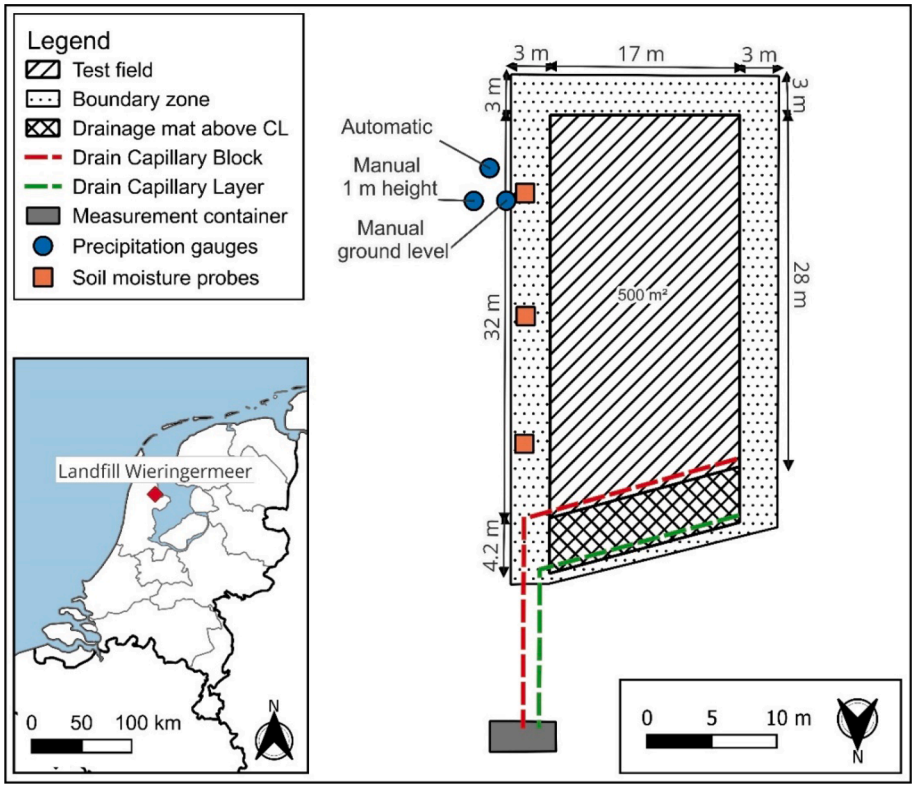


Fig. 2. Location (52.77° N, 5.08° E) and top view of the test field. Distances are given parallel to the slope and the area is given horizontally. The base of landfill is located at −5 m above sea level.

Table 1
Soil properties of the different layers and fitted van Genuchten (1980) parameters. Gravel, sand, silt and clay are defined as particles larger than 2 mm, between 0.063 and 2 mm, between 0.002 and 0.063 mm and smaller than 0.002 mm, respectively. Data from melchior + wittpohl Ingenieurgesellschaft (2009, 2011, 2014).

Layer	Topsoil	Subsoil	Capillary layer	Capillary block
Layer thickness (m)	0.2	0.9	0.3	0.2
Proctor density (kg/m^3)	1.604	1.728	1.709	1.631
Average bulk density (g/cm^3)	1.214	1.369	1.502	1.601
Gravel (mass-%)	3.0	3.1	4.0	98.6
Sand (mass-%)	43.2	78.0	95.7	1.3
Silt (mass-%)	40.5	8.9	0.3	0.1
Clay (mass-%)	13.3	10.0	0.0	0.0
Total organic carbon(mass-%)	4.4	2.3	0.2	0.6
Saturated hydraulic conductivity (m/s)	4.5×10^{-5}	4.8×10^{-5}	6.2×10^{-5}	2.7×10^{-2}
Porosity, θ_s (m^3/m^3)	0.51	0.47	0.42	0.46
α (1/kPa)	0.64	1.57	0.71	–
n (–)	1.20	1.22	1.62	–
θ_r (m^3/m^3)	0.06	0.08	0.00	–

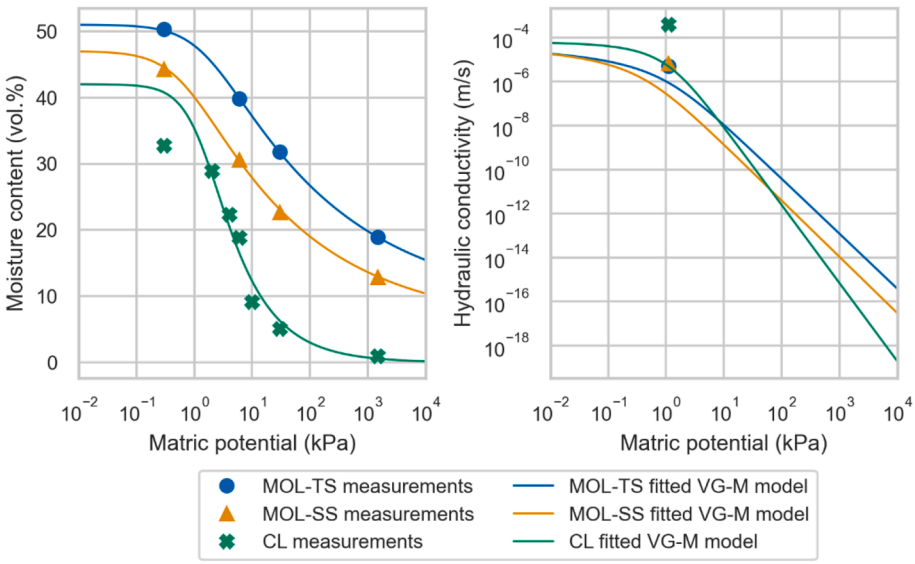


Fig. 3. Left: Average water retention curves of the top and subsoil of the methane oxidation layer (MOL-TS, MOL-SS, respectively) and the capillary layer (CL), measured after construction in 2009 with a fitted van Genuchten-Mualem (VG-M) model (Mualem, 1976; van Genuchten, 1980). Right: Estimation of the hydraulic conductivity as function of matric potential given by the fitted van Genuchten-Mualem model and the saturated hydraulic conductivities presented in Table 1, including geometrically averaged hydraulic conductivities of each layer at 1 kPa (melchior + wittpohl Ingenieurgesellschaft., 2014).

2.1.2. Soil properties

Various soil physical properties of the methane oxidation layer were measured in 2009 and 2011 and before and after the compaction in 2013 (Table 1). The capillary layer and block were analysed only in 2009. Grain size distribution was determined using a wet sieving test, following the German standard DIN 18123, and soil moisture retention properties were measured using pressure plate tests (German standard DIN ISO 11274; Fig. 3). Saturated and unsaturated hydraulic conductivities were obtained using a falling head test in the laboratory and the method developed by Ankeny et al. (1988) in the field, respectively. A spreadsheet containing the measurements can be found at DOI: 10.4121/1900c71a-9980-4848-81bb-6815e4478b2c.

A van Genuchten-Mualem model (Mualem, 1976; van Genuchten, 1980) was fitted on the water retention data using the RETC-software (van Genuchten et al., 1991). The parameters α, n and θ_r were fitted, using the porosity as saturated water content (θ_s) and assuming $m = 1 - \frac{1}{n}$. This yielded an estimate for the hydraulic conductivity as function of matric potential (Fig. 3).

The topsoil classifies as loam and the subsoil in the methane oxidation layer as loamy sand (Food and Agriculture Organization of the United Nations, 2014). The latter also has a relatively coarse texture and high hydraulic conductivity due to its high air-filled porosity, resulting from its optimisation for methane oxidation. The material of the capillary layer classifies as coarse sand (Food and Agriculture Organization of the United Nations, 2014) and the capillary block is comprised of gravel.

Based on laboratory experiments, the design diversion capacity of the capillary layer was approximately 20 mm/d. Although filter stability was considered during the design of the field (melchior + wittpohl Ingenieurgesellschaft, 2008), an excavation in 2017 found sand in the capillary block (van Verseveld, 2018). Furthermore, this excavation revealed the formation of a thin layer of iron precipitates at the bottom 3 cm of the capillary layer (Supplementary material section S.4). Further details on the test field setup, construction and soil properties can be found in Geck et al. (2016) and Röwer et al., (2016a).

2.2. Local climatic conditions

The precipitation, reference crop evapotranspiration (ET_{ref}) and temperature measured at the Royal Netherlands Meteorological Institute (KNMI) weather station at De Kooy between 1980 and 2010 were analysed to characterise the local climate (KNMI, 2023a). This was the closest weather station (25 km away from the test field) with measurements in that time period.

The reference crop evapotranspiration provided by the KNMI is an estimate of evapotranspiration of a soil covered with optimally growing grass without shortage of water under the prevailing weather conditions (De Bruin, 1987). This estimate is based on the expression of Makkink & Heemst (1967) which uses temperature and the daily sum of global radiation and is only applicable on a regional scale between March and October (De Bruin, 1987).

2.3. Test field water balance

The water balance of the test field was analysed on both daily and annual scale. An overview of the data used per analysis is given in the supplementary material (section S.5) and the data and processing scripts are published at https://doi.org/10.4121/1900c71a-9980–4848-81bb-6815e4478b2c.

2.3.1. Daily water balance

The water balance of the test field (Fig. 1) on a daily scale was defined as:

$$\Delta S = P - ET_a - Q_{cl} - Q_{cb} \quad (1)$$

where ΔS denotes the change in water storage (mm/d), P the precipitation (mm/d), ET_a the actual evapotranspiration (mm/d) and Q_{cl} and Q_{cb} denote the outflows from the capillary layer and capillary block respectively (mm/d). On-site precipitation observations were characterized by many gaps and were only used to analyse the short-term hydraulic behaviour on hourly scale, which is not considered in this paper. Instead, the hourly precipitation data of the KNMI weather station at Berkhout (16 km away from the test field) between November 2009 and April 2023 were used (KNMI, 2023b). Daily outflows were derived from the outflow measurements (see section 2.3.3). Evapotranspiration and the change in water storage were not measured directly. Instead, these were approximated by the measured volumetric water contents (see section 2.3.3) and the reference evapotranspiration provided by the KNMI, multiplied with a crop factor of 1 because of the test fields' grass vegetation cover (Feddes, 1987).

2.3.2. Annual water balance

Observations of the soil moisture between 2010 and 2014 showed that the water content at the start of April is approximately equal each year. Hence, April was chosen as the start of the hydrological year to analyse the annual water balance and the change in stored water was assumed to be zero:

$$\Delta S = P - ET_a - Q_{cl} - Q_{cb} \approx 0 \quad (2)$$

With ΔS the change in stored water (mm/a), P the precipitation (mm/a), ET_a the evapotranspiration (mm/a) and Q_{cl} and Q_{cb} the outflow from the capillary layer and block respectively (mm/a). As the outflows (see section 2.3.3) and the precipitation (KNMI station Berkhout) were measured, the residual of the annual water balance was then assumed to reflect the yearly evaporation.

2.3.3. Measurements of outflow and water storage

The outflows from the capillary layer and capillary block were measured between November 2009 and April 2023. They were recorded using 3 L tipping buckets (Umweltanalytische Produkte GmbH), and tipping events were registered automatically. Bucket volume was re-calibrated monthly to account for any volume reduction by precipitates in the outflow. If necessary, the buckets were cleaned. In this study, the average bucket volume was used for the whole timeseries. The tipping buckets discharged into 1 m^3 tanks which were emptied by RS-100 pumps (230 V, 25 mm outlet, German Water and Energy Group GmbH). The number of pump switches combined with the pump volume per switch (0.5 m^3) served to cross-check the flow volumes estimated using the tipping bucket data. The two timeseries were in good accordance with each other, except for the period 23–03-2013 to 05–10-2013 and 19–03-2022 to 04–05-2022 for the capillary layer (Supplementary material section S.6). For these periods, the tipping bucket flow was therefore omitted for the analysis on daily scale and replaced by the pump flow for the analysis on a yearly scale. Due to power or network failures, the recording of discrete outflow events was sometimes disturbed. However, the data were stored cumulatively, so the total flow over the no-data period was preserved, resulting in a larger discrete flow for the day after a no-data period. Therefore, these days were not considered for the analysis of daily flow patterns, but were included in the analysis of the yearly time scale.

Volumetric water contents were measured between May 2010 and October 2014 at 5, 15, 40 and 80 cm depth at up-, mid- and downslope positions (Fig. 1) using frequency domain reflectometry probes (ECH2O EC-5, Decagon) connected to a data-logging unit (Supplementary material section S.7). Data were recorded at an interval of 15 min.

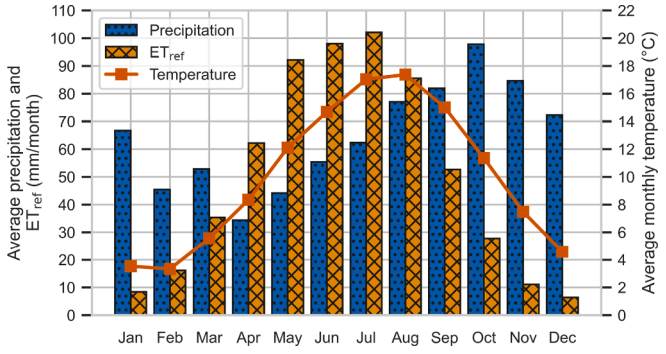


Fig. 4. Average monthly precipitation, reference crop evapotranspiration (ET_{ref}) and temperature for the period 1980 to 2010. Analysis based on data from weather station De Kooy from the Royal Netherlands Meteorological Institute.

3. Results

3.1. Local climatic conditions

The local climate can be described as a maritime temperate climate (Cfb; Beck et al., 2018; Köppen, 1884). The average annual precipitation and reference crop evapotranspiration between 1980 and 2010 at weather station De Kooy were 750 and 580 mm/a, respectively. Average monthly precipitation during that period follows a slight seasonal pattern, with more rain from October to December than from April to June (Fig. 4). The seasonal pattern of the average temperature is much stronger and ranges from approximately 3.5 °C in February to 17 °C in August. Along with the temperature, the reference crop evapotranspiration ranges from less than 10 mm/month in January and December to approximately 100 mm/month in July. On average, there is thus a precipitation surplus from September to March which can be as large as 70 mm/month. Conversely there is a precipitation deficit between April and August of up to 30 mm/month. Moreover, likely due to climate change, the annual precipitation, reference crop evapotranspiration and temperature increased after 2010, but the seasonal pattern remained similar (van Dorland et al., 2023).

3.2. Annual water balance and capillary barrier flows

The yearly precipitation in the study period ranged from 699 mm/a in 2018 to 1011 mm/a in 2017, averaging 848 mm/a (Fig. 5). In general, 55–65 % of the precipitation evaporated, except for drier years when it reached up to 74 % (2016). Compared to the precipitation, the variation in evaporation was little and ranged between 459 mm/a in 2010 to 564 mm/a in 2017, with an average of 504 mm/a (59 % of the precipitation). Breakthrough averaged around 62 mm/a (7.3 % of the precipitation), with a range from 20 (2010, 2016) to 80 mm/a (2019). In 2012, an exceptional breakthrough of 162 mm/a was observed, which equals 16 % of the precipitation in that year. Drier years, such as 2010 and 2016, showed breakthrough amounts of approximately 20 mm/a. Diverted infiltration exhibited a relatively large spread compared to the relative spread in evaporation and breakthrough, ranging from 167 mm/a in 2016 to 375 mm/a in 2017, with an average annual value of 282 mm/a. In general, the equivalent of 31–36 % of the precipitation was diverted by the barrier. Lower fractions were observed in the dry years 2016 (23 %) and 2018 (26 %). On average, the capillary barrier successfully deviated 82 % of the inflow into the capillary barrier.

3.3. Daily capillary barrier outflows

The outflow from the capillary layer and the capillary block both exhibited strong seasonal variability (Fig. 6). Days with outflow occured mainly when the evapotranspiration was low. Generally, in the summer half-year (April-September) precipitation is evaporated from or stored in the cover soil and hence does not reach the capillary barrier. In the winter half-year (October-March), the storage capacity of the cover soil is exceeded, and the soil transmits the precipitation to the capillary barrier, inducing discharge from the latter. These conditions can also occur outside the winter half-year, of which April 2018 is an example.

Furthermore, the outflow from both layers showed characteristic behaviour of a flow peak followed by an exponential decay upon inflow of water. The flow peaks were higher and the decay times were shorter for the capillary block than for the capillary layer. Discharge from both layers combined reached up to 16 mm/d. For both layers, 45 % of the total discharge in the measurement period was caused by flows of more than 2 mm/d (Supplementary material section S.8). Of the total 4582 days with valid capillary block flow measurements, only 498 (10 %) were without any breakthrough, whereas on approximately 70 % of the days, there was a flow between 0 and 0.1 mm/d, which made up for 10 % of the total breakthrough.

Over the time of the field trial, breakthrough occurred at different

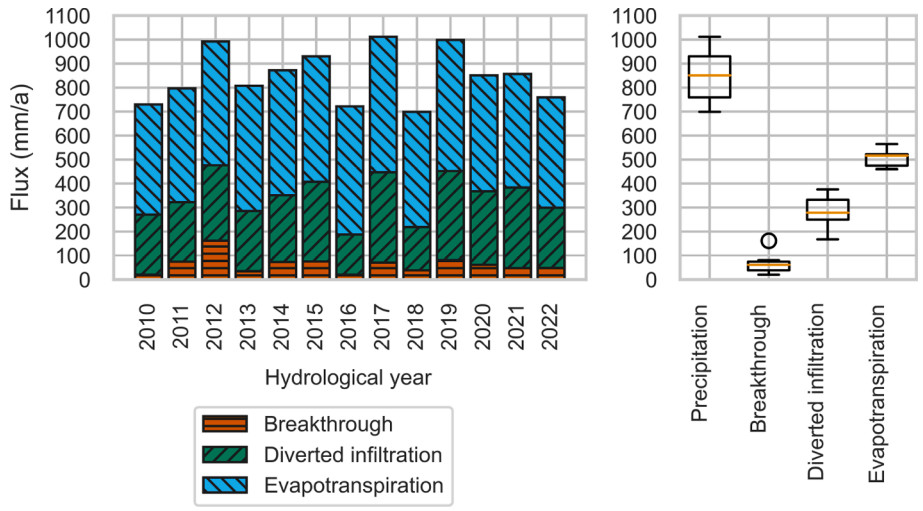


Fig. 5. Left: Annual water balance. Right: Boxplot of the annual precipitation, diverted infiltration, breakthrough and evapotranspiration of the left graph. Box spans first, second (orange line) and third quartile which is the inter-quartile range (IQR). Whiskers extend to highest/lowest value within 1.5*IQR. Data beyond this range are plotted as points. (For interpretation of the references to colour in this figure legend, the reader is referred to the web version of this article.)

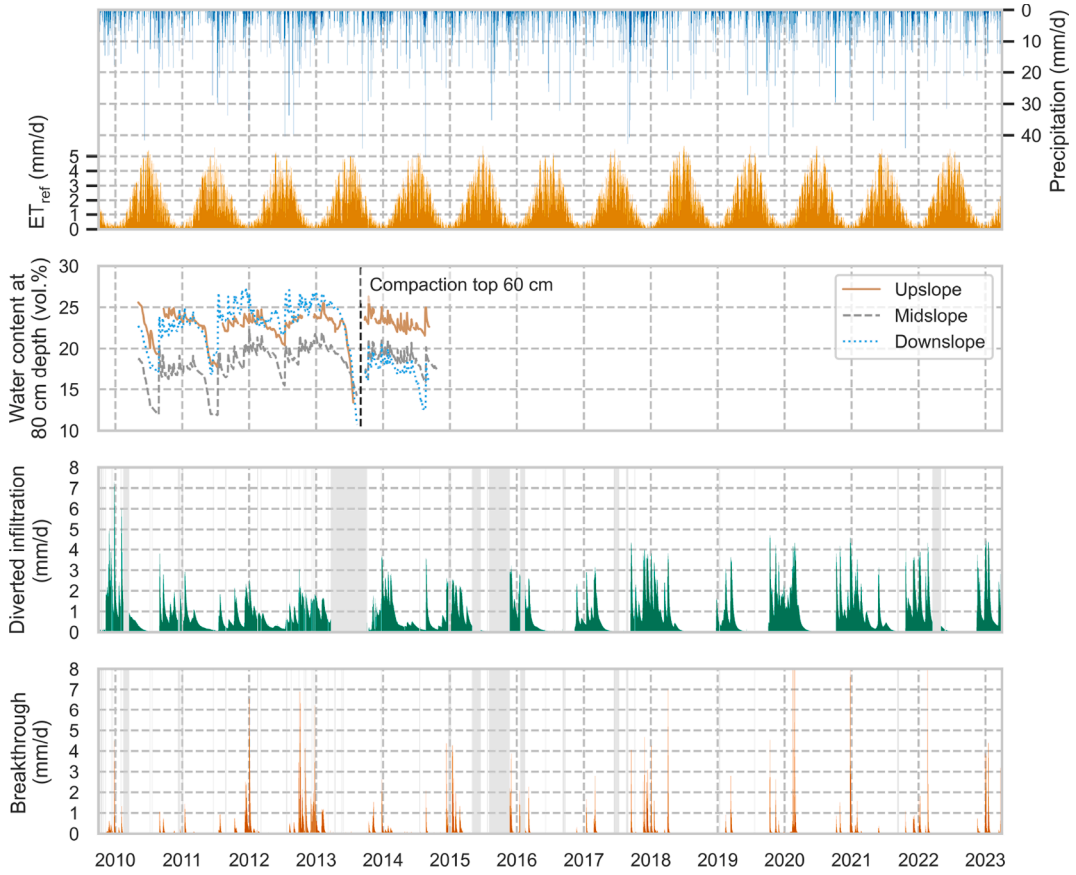


Fig. 6. Daily precipitation, reference crop evapotranspiration, water content at 80 cm depth, diverted infiltration (capillary layer outflow) and breakthrough (capillary block outflow). Periods without data are indicated by grey shading.

discharge rates from the capillary layer, indicating a change in the diversion capacity of the capillary barrier (Fig. 7). Initially, major breakthrough of more than 1 mm/d occurred at a diversion capacity of 6 mm/d. In 2010, the diversion capacity drastically decreased to approximately 2 mm/d. The diversion capacity increased again to approximately 4 mm/d in the years after.

Before the compaction of the top 60 cm of the cover soil in 2013, the water content at 80 cm depth was similar for the up and downslope positions. The midslope observations show a similar trend, but generally were lower by ~ 5 vol%. After the compaction of the top 60 cm in 2013, the mid and downslope moisture contents were similar, and the upslope observations showed a positive offset. These differences are likely due to local differences in soil water retention in relation to heterogeneity in soil compaction during test field construction and the compaction in

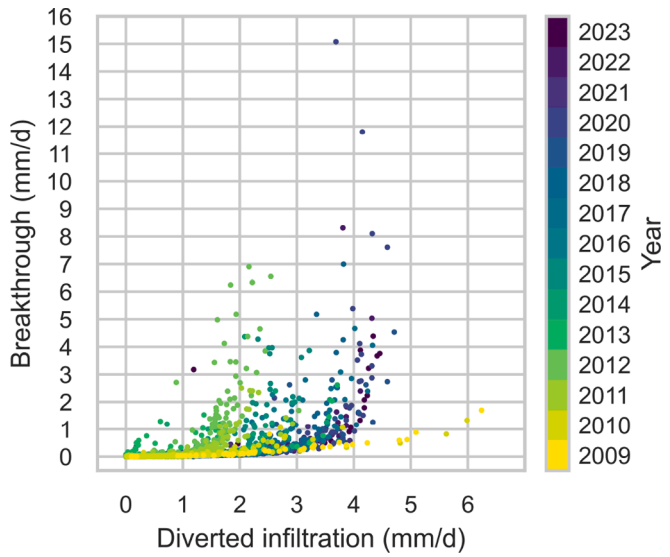


Fig. 7. Relationship between daily outflows from the capillary barrier (breakthrough) and the capillary layer (diverted infiltration), clustered by year of measurement.

2013 or to heterogeneity of the methane oxidation layer material, for example, by aggregation (Supplementary material section S.4).

On 17–02-2020 and 24–12-2020 the breakthrough exceeded 8 mm/d, amounting to 11.8 and 15.1 mm/d, respectively.

4. Discussion

4.1. Potential errors in the annual water balance

The potential errors in the components of the annual water balance were considered insignificant for the total water balance. The error in the precipitation measurements has an order of magnitude of only 10^{-3} mm/d (Kuik, 2001). Also, KNMI estimated the difference in average annual precipitation amount between the Berkhout station and the test field to be less than 5 mm per year (Wolters et al., 2011). Furthermore, the average difference between the annual outflow measured by the tipping buckets and the pumps was 14.9 and 3.2 mm/a for the capillary layer and block, respectively, amounting to approximately 5 % of the annual flow volume (Supplementary material section S.6).

The annual water balance residual was used as an estimate of the evapotranspiration and includes the uncertainties related to precipitation and outflow (see above), the change in stored moisture over each year, and the possibility of subsurface in and outflow from the test field in the methane oxidation layer. The absolute difference between the water content at the start and the end of each year, based on the data collected between 2010 and 2014, averaged for each layer over the three locations along the slope, amounted to an average of 20 mm, i.e. approximately 4 % of the yearly average water balance residual (Supplementary material section S.9). Concerning the subsurface flow, a vertical HDPE bund extending to the top of the capillary barrier precluded lateral inflow of water into the capillary barrier itself (Fig. 1). Potential interflow within the methane oxidation layer, if at all happening, was assumed to be net zero for the total of the test field area, as the potential inflow at the upper boundary would equal the potential outflow at the lower boundary. The assumption is based on the fact that due to the construction of a boundary zone with identical soil properties around the test field, the soil properties can be considered similar within and outside of the field at both positions along the slope. Similarly, a capillary effect between the methane oxidation layer and the capillary layer was considered negligible as the cover soil commonly had a water content of approximately 23 vol-% (Fig. 6), which corresponds approximately to the water entry value of the capillary layer (approximately 30 kPa; Fig. 3). So, the error in the evaporation estimate was considered negligible. The yearly water balance residual amounted to 475–525 mm/a (55–65 % of the precipitation), which is similar to the annual evapotranspiration measured elsewhere in the Netherlands and on a test field in Northern Germany under comparable climatic conditions (Elbers et al., 2009; Melchior et al., 2010).

4.2. Annual performance of the capillary barrier system

On average, the capillary barrier diverted 282 mm/a (equivalent to 33 % of the annual precipitation), which equals 82 % of the infiltration reaching the capillary barrier. Variability in annual precipitation is mainly reflected in variability in diverted infiltration. However, the absolute average annual breakthrough in this study (62 mm/a; 7.3 % of precipitation) exceeds the currently accepted seepage rate into a waste body of 5 mm/a in the Netherlands (Ministerie van Volkshuisvesting, Ruimtelijke Ordening en Milieubeheer, 1991). The German landfill ordinance (DepV, 2009) stipulates a maximum of 10 to 30 mm/a, depending on the hazard class of the landfill, and the European Landfill Directive accepts a maximum of 30 mm/a (Council Directive, 1999/31/EC on the Landfill of Waste, 1999). As expected, based on the annual precipitation and evaporation patterns, the system performance occurred was poorer mainly in the winter half-year (October-March). As Geck et al. (2016) observed that colder and moister conditions also impeded the methane oxidation efficiency of the cover soil in the test field, the winter period is critical to both aspects of this dual functionality cover system. Concerning the hydraulic performance during this period, during which the storage of the methane oxidation layer was exceeded, the occurrence of breakthrough is determined by the inflow rate of the infiltrating water into the capillary barrier, controlled by the hydraulic properties of the cover soil, and the diversion capacity of the capillary barrier.

4.3. Permeability of the cover soil

Field studies of cover designs where the capillary barrier was protected from high inflow rates performed better than the system in this study. The capillary barriers in the field studies of Melchior et al. (2010) (Hamburg, Germany) and Giurgea et al. (2003) (Karlsruhe, Germany), which were subject to comparable climatic conditions as in this study, diverted 90 and 93 % of the total infiltration reaching the capillary barrier, respectively. The combination of a drainage and thick less permeable clay layer diverted most of the precipitation so that only 12 % (Giurgea et al., 2003) and 16 % (Melchior et al., 2010) of the annual precipitation reached the capillary barrier, protecting it from high hydraulic loads, even after deterioration of the clay layer by crack formation in dry periods. Consequently, less breakthrough amounts were observed. Melchior et al. (2010) reported an average annual breakthrough of 16 mm/a (1.8 % of precipitation), and Giurgea et al. (2003) observed 7 mm/a of breakthrough (0.8 % of precipitation). A field study in Quebec (Canada), where precipitation and evapotranspiration on average amount to approximately 1200 and 400 mm/a, respectively (Wang et al., 2013), showed an average annual breakthrough of only 8 mm/a (0.7 % of the precipitation equivalent; Abdolahzadeh et al., 2011). The capillary barrier in this cover design was also protected by a low permeable layer.

In contrast, the cover soil used in this study has a hydraulic conductivity at saturation and at 1 kPa matric potential of an order of magnitude of 10^{-5} and 10^{-6} m/s, respectively (Fig. 3). This relatively high conductivity results from the optimisation of the soil for its gas transport properties, required to satisfy the methane oxidation function, and also from requirements regarding slope stability. The soil's properties were unique in that regard, as the soil combined a relatively high moisture retention capacity with a high hydraulic conductivity (classification according to Ad-hoc Arbeitsgruppe Boden, 2005). As a result,

the inflow rates were significantly higher than the diversion capacity of the capillary barrier, leading to breakthrough of up to 15 mm/d.

Recently, Ng et al. (2021) investigated the performance of a cover design with a low permeable layer beneath the capillary barrier to make the system capable of diverting the high precipitation in a humid regions like in Hong Kong. During a four-year field test, on average 24 mm/a of precipitation percolated through the cover. Also, Zhan et al., (2020a) tested a two-layer cover design consisting of a loess capillary layer on top of a gravel capillary block in Xi'an (China). Only 16 mm of the approximately 1000 mm precipitation in the two-year observation period percolated through the cover. This cover design also showed promising results regarding methane oxidation (Zhan et al., 2020b). However, the climate at the location of these studies is much different with an annual evapotranspiration higher than the precipitation and the rainy season coinciding with a period of high temperatures and evapotranspiration, making an intercomparison with these studies difficult.

As a consequence of the dual functionality design, the methane oxidation layer did not hydraulically protect the capillary barrier as well as the low permeability layers in the studies of Giurgea et al. (2003), Melchior et al. (2010) and Abdolahzadeh et al. (2011). However, such a layer would form an obstruction for gas transport and reduce methane oxidation, which was also the case for the cover design tested by Ng et al. (2021). This precludes the implementation of these concepts in a methane oxidation system. Nevertheless, reducing the hydraulic conductivity of the methane oxidation layer and thereby possibly compromising on its gas transport properties could improve the hydraulic aspect of the cover design. This could be done by increasing the share of finer particles in the soils used for the methane oxidation layer (Mahmoodlu et al., 2016). Increasing the depth of the methane oxidation layer could also reduce the hydraulic load into the capillary barrier due to a longer travel time of the soil percolate.

Although the hydraulic conductivity of the methane oxidation layer decreased and gas distribution at its base became more even (Geck et al., 2016) after compaction of the upper decimeters in 2013, its effect on the system's overall hydraulic performance was estimated to be negligible. The soil water volumetric water content measurements (Supplementary material section S.7) indicated that saturation was rarely reached in the test field. The compaction primarily decreased the amount of coarse pores (van Verseveld & Gebert, 2020), which are less relevant for unsaturated flow. This is also suggested by the smaller reduction in hydraulic conductivities at 1 kPa matric potential compared to the saturated hydraulic conductivities (Supplementary material section S.3).

4.4. Diversion capacity of the capillary barrier

The capillary barrier's design diversion capacity of 20 mm/day would have been suited to manage the hydraulic load from the methane oxidation layer. However, the actual diversion capacity in the test field consistently fell short of this design capacity. This can be attributed to heterogeneities introduced by the construction with large machines which can lead to changes in the granular matrix, affecting its hydraulic properties, inducing local breakthrough and a reduction of the diversion capacity (Ho & Webb, 1998).

The diversion capacity of the capillary barrier exhibited a dynamic behaviour, showing after a sharp decrease from approximately 6 to 2 mm/d in 2010, and a steady increase to 4 mm/d over the subsequent years. This increase in diversion capacity over time explains why the annual breakthrough in 2012 was double the amount of the breakthrough registered in 2017 and 2019 when annual precipitation amounts were similar. Nevertheless, the diversion capacity of the test field in this study before 2010 (6 mm/d) and after 2018 (4 mm/d) is relatively high compared to the capacities in the field studies of Giurgea et al., (2003; 1 mm/d) and Kämpf & Montenegro (1997; 2.8 mm/d). The excavation in 2017 showed the presence of a saturated capillary seam (as also reported by Kämpf et al., 2003), the formation of iron precipitates at the upper boundary of the capillary seam (Supplementary material section S.4), and the presence of sand particles in the capillary block. It is hypothesised that in 2010, although filter stability was taken into account during design, suffusion led to an infiltration of sand particles from the capillary layer into the capillary block, increasing its water entry value and hence decreasing the diversion capacity of the capillary barrier. The extent and, hence, the possible effect of the particle dislocation is unknown. The subsequent steady increase of the diversion capacity after 2013 is suspected to be due to further suffusion into deeper layers of the capillary block, driving the sand particles away from the interface with the capillary layer, thereby again decreasing the water entry value of the capillary block and improving the diversion capacity of the capillary barrier.

The observed iron precipitates indicated a boundary between reducing (saturated) and oxidising (unsaturated) conditions and were likely formed from iron released from the cover soil. Iron-rich percolate and corresponding iron precipitates at the test field's outflow were also observed from the neighbouring test field constructed with the same cover soil. In that field, the functionality of a stormwater drainage mat underlying the cover soil was tested for diversion of water as an alternative to the capillary barrier. The formation of iron precipitates is suspected to have increased the stability of the remaining sand particles, decreasing suffusion. On the other hand, the iron precipitates could also have induced an opposite effect by decreasing the hydraulic conductivity in the saturated seam of the capillary layer, thereby reducing its diversion capacity (Kämpf et al., 2003), and increasing its moisture retention, enhancing breakthrough as the water entry value of the capillary block would have been reached faster.

Lastly, the high number of days (70 %) with capillary block flows between 0 and 0.1 mm/d could be explained by steady uniform seepage through the capillary barrier as observed by Kämpf et al. (2003) in their laboratory study. This corresponds with the film phase flow described by Scarfone et al. (2020) and Steinert (1999). These flows entail 10 % of the total breakthrough amount and cannot be easily prevented, which makes this an important phenomenon to take into account when designing landfill cover systems containing capillary barrier systems.

5. Conclusions

This study presented a field test of a dual-functionality landfill cover which combines methane oxidation and infiltration diversion with a capillary barrier. The long term field hydraulic performance of this design was promising but requires refinement. Over 13 years, on average, 59 %, 33 % and 7 % of the precipitation (848 mm/a) evaporated, was diverted and percolated through the cover, respectively. The capillary barrier diverted 82 % of the water percolating through the methane oxidation layer. As expected, the system failed mainly in the winter half-year (October-March) when precipitation exceeded evapotranspiration. Compared to other field studies, the permeability of the cover soil or methane oxidation layer was high, leading to a relatively higher inflow rate of infiltration into the underlying capillary barrier during that period. In contrast, the diversion capacity of the capillary barrier was also relatively high initially, but it decreased after one year of operation, leading to higher breakthrough amounts. The decrease was followed by a partial restoration of the diversion capacity, in 2023 reaching up to approximately 66 % of the original value. Possible explanations for the deterioration of the diversion capacity are the suffusion of sand from the capillary layer into the capillary block and subsequent washout to greater depths and the potential influence of iron precipitates at the interface between the capillary layer and block. However, more research is needed to identify the cause of this dynamic behaviour as maintaining a stable diversion capacity is crucial for the performance of this dual-functional landfill cover configuration in a temperate climate. Follow-up research could also investigate the effect of using a soil with a higher share of fine particles for the methane oxidation layer on the hydraulic and methane oxidation performance.

Funding sources

Construction and operation of the test fields was funded by N.V. Afvalzorg Holding, the Dutch Sustainable Landfill Foundation (SDS) and SenterNovem (now the Netherlands Enterprise Agency RVO; project no. ROBS090111).

CRediT authorship contribution statement

J.M. van den Brink: Writing – original draft, Visualization, Project administration, Methodology, Formal analysis, Data curation, Conceptualization. **H. Scharff:** Writing – review & editing, Resources, Methodology, Investigation, Funding acquisition, Data curation, Conceptualization. **B. Steinert:** Writing – review & editing, Resources, Methodology, Conceptualization. **S. Melchior:** Writing – review & editing, Resources, Methodology, Conceptualization. **M. Hrachowitz:** Writing – review & editing, Validation, Conceptualization. **T.J. Heimovaara:** Writing – review & editing, Validation, Methodology, Conceptualization. **J. Gebert:** Writing – review & editing, Writing – original draft, Supervision, Resources, Project administration, Methodology, Investigation, Conceptualization.

Declaration of competing interest

The authors declare that they have no known competing financial interests or personal relationships that could have appeared to influence the work reported in this paper.

Data availability

The method section contains a link to the data and code used at the end of paragraph 2.5.

Acknowledgements

The authors thank Dr. Susan Yi for language-proofing the manuscript.

Appendix A. Supplementary material

Supplementary data to this article can be found online at https://doi.org/10.1016/j.wasman.2024.07.002.

References

Abdolahzadeh, A.M., Vachon, B.L., Cabral, A.R., 2011. Evaluation of the effectiveness of a cover with capillary barrier effect to control percolation into a waste disposal facility. Can. Geotech. J. 48 (7), 996–1009. https://doi.org/10.1139/t11-017.

Ad-hoc Arbeitsgruppe Boden. (2005). *Bodenkundliche Kartieranleitung* (5th ed.). Bundesanstalt für Geowissenschaften und Rohstoffe in Zusammenarbeit mit Geologische Landesämter der Bundesrepublik Deutschland.

Ahoughalandari, B., Cabral, A.R., 2017. Influence of capillary barrier effect on biogas distribution at the base of passive methane oxidation biosystems: parametric study. Waste Manag. 63, 172–187. https://doi.org/10.1016/j.wasman.2016.11.026.

Ankeny, M.B., Kaspar, T.C., Horton, R., 1988. Design for an automated tension infiltrometer. Soil Sci. Soc. Am. J. 52, 893–896. https://doi.org/10.2136/sssaj1988.03615995005200030054x.

Aubertin, M., Cifuentes, E., Apithy, S.A., Bussière, B., Molson, J., Chapuis, R.P., 2009. Analyses of water diversion along inclined covers with capillary barrier effects. Can. Geotech. J. 46 (10), 1146–1164. https://doi.org/10.1139/T09-050.

Baker, R.S., Hillel, D., 1990. Laboratory tests of a theory of fingering during infiltration into layered soils. Soil Sci. Soc. Am. J. 54 (1), 20–30. https://doi.org/10.2136/sssaj1990.03615995005400010004x.

Beck, H.E., Zimmermann, N.E., McVicar, T.R., Vergopolan, N., Berg, A., Wood, E.F., 2018. Present and future köppen-geiger climate classification maps at 1-km resolution. Sci. Data 5, 1–12. https://doi.org/10.1038/sdata.2018.214.

Berger, J., Fornés, L.V., Ott, C., Jager, J., Wawra, B., Zanke, U., 2005. Methane oxidation in a landfill cover with capillary barrier. Waste Manag. 25, 369–373.

Brand, E., de Nijs, T.C.M., Dijkstra, J.J., Comans, R.N.J., 2016. A novel approach in calculating site-specific aftercare completion criteria for landfills in The Netherlands: Policy developments. Waste Manag. 56, 255–261. https://doi.org/10.1016/j.wasman.2016.07.038.

De Bruin, H.A.R., 1987. From Penman to Makkink. In: Hooghart, J.C. (Ed.), Evaporation and Weather. Netherlands Organisation for Applied Scientific Research TNO, pp. 5–31.

DepV. (2009). *Deponieverordnung vom 27. April 2009 (BGBl. I S. 900), die zuletzt durch Artikel 3 der Verordnung vom 9. Juli 2021 (BGBl. I S. 2598) geändert worden ist*. https://www.gesetze-im-internet.de/depv_2009/DepV.pdf.

Council Directive 1999/31/EC on the landfill of waste, Official Journal of the European Communities L182/1 (1999).

Elbers, J.A., Moors, E.J., Jacobs, C.M.J., 2009. Gemeten actuele verdamping voor twaalf locaties in Nederland. Alterra.

Feddes, R. A. (1987). Crop factors in relation Makkink reference crop evapotranspiration. In J. C. Hooghart (Ed.), *Evaporation and weather* (pp. 33–46). Netherlands Organisation for Applied Scientific Research TNO.

Food and Agriculture Organization of the United Nations. (2014). *World Reference Base for Soil Resources 2014: International Soil Classification System for Naming Soils and Creating Legends for Soil Maps*. Food and Agriculture Organization.

Gebert, J., Huber-Humer, M., Cabral, A.R., 2022. Design of microbial methane oxidation systems for landfills. Front. Environ. Sci. 10 https://doi.org/10.3389/fenvs.2022.907562.

Geck, C., Scharff, H., Pfeiffer, E.M., Gebert, J., 2016. Validation of a simple model to predict the performance of methane oxidation systems, using field data from a large scale biocover test field. Waste Manag. 56, 280–289. https://doi.org/10.1016/j.wasman.2016.06.006.

Giurgea, V. I., Hötzl, H., & Breh, W. (2003). Studies on the long-term performance of an alternative surface-sealing system with underlying capillary barrier. In T. H. Christensen, R. Cossu, & R. Stegmann (Eds.), *Ninth International Waste Management and Landfill Symposium*. CISA, Environmental Sanitary Engineering Centre.

Ho, C.K., Webb, S.W., 1998. Capillary barrier performance in heterogeneous porous media. Water Resour. Res. 34 (4), 603–609. https://doi.org/10.1029/98WR00217.

Huber-Humer, M., Gebert, J., Hilger, H., 2008. Biotic systems to mitigate landfill methane emissions. Waste Manag. Res. 26 (1), 33–46. https://doi.org/10.1177/0734242X07087977.

Kämpf, M., Holfelder, T., Montenegro, H., 2003. Identification and parameterization of flow processes in artificial capillary barriers. Water Resour. Res. 39 (10), 1276–1285. https://doi.org/10.1029/2002WR001860.

Kämpf, M., Montenegro, H., 1997. On the performance of capillary barriers as landfill cover. Hydrol. Earth Syst. Sci. 4, 925–929.

Khire, M.V., Benson, C.H., Bosscher, P.J., 1999. Field data from a capillary barrier and model predictions with UNSAT-H. J. Geotech. Geoenviron. Eng. 125 (6), 518–527.

Khire, M.V., Benson, C.H., Bosscher, P.J., 2000. Capillary Barriers: Design Variables and Water Balance. J. Geotech. Geoenviron. Eng. 126 (8), 695–708.

[dataset] KNMI. (2023a). *Daggegevens van het weer in Nederland*. Retrieved October 19th, 2023, from https://www.knmi.nl/nederland-nu/klimatologie/daggegevens.

[dataset] KNMI. (2023b). *Uurgegevens van het weer in Nederland*. Retrieved October 19th, 2023, from https://www.knmi.nl/nederland-nu/klimatologie/uurgegevens.

Köppen, W., 1884. Die Wärmezonen der Erde, nach der Dauer der heissen, gemässigten und kalten Zeit und nach der Wirkung der Wärme auf die organische Welt betrachtet. Meteorol. Z. 1, 215–226.

Kuik, F. (2001). *Neerslagonderzoek 1998*. KNMI. Retrieved December 21st from https://www.knmi.nl/knmi-bibliotheek/publicaties/intern-rapport.

Li, X., Li, X., Wang, F., Liu, Y., 2022. The design criterion for capillary barrier cover in multi-climate regions. Waste Manag. 149, 33–41. https://doi.org/10.1016/J.WASMAN.2022.06.002.

Mahmoodlu, M.G., Raoof, A., Sweijen, T., van Genuchten, M.T., 2016. Effects of sand compaction and mixing on pore structure and the unsaturated soil hydraulic properties. Vadose Zone J. 15 (8), 1–11. https://doi.org/10.2136/vzj2015.10.0136.

Makkink, G.F., van Heemst, H.D.J., 1967. De potentiële verdamping van kort gras en water. Jaarboek IBS 89–96.

melchior + wittpohl Ingenieurgesellschaft. (2008). *Versuchfelder Deponie Nauerna Materialuntersuchungen Kapillarsperre und Methanoxidationsschicht: Abschlussbericht*.

melchior + wittpohl Ingenieurgesellschaft. (2009). *Versuchsfelder Deponie Wieringermeer Bauüberwachung und Prüfung mineralische Baustoffe Abschlussdokumentation*.

melchior + wittpohl Ingenieurgesellschaft. (2011). *Versuchsfelder Deponie Wieringermeer Aufgrabung 2011 Ergebnisbericht*.

melchior + wittpohl Ingenieurgesellschaft. (2014). *Versuchsfelder Deponie Wieringermeer Aufgrabungen 2013 Ergebnisbericht*.

Melchior, S., Sokollek, V., Berger, K., Vielhaber, B., Steinert, B., 2010. Results from 18 years of in situ performance testing of landfill cover systems in Germany. J. Environ. Eng. 136 (8), 815–823. https://doi.org/10.1061/(asce)ee.1943-7870.0000200.

Melchior, S. (1993). *Wasserhaushalt und Wirksamkeit mehrschichtiger Abdecksysteme für Deponien und Altlasten*. [PhD theses, Universität Hamburg].

Mualem, Y., 1976. A new model for predicting the hydraulic conductivity of unsaturated porous media. Water Resour. Res. 12 (3) https://doi.org/10.1029/WR012i003p00513.

Ng, C.W.W., Guo, H.W., Xue, Q., 2021. A novel environmentally friendly vegetated three-layer landfill cover system using construction wastes but without a geomembrane. Indian Geotech. J. 51 (3), 460–466. https://doi.org/10.1007/s40098-021-00542-7.

Oldenburg, C.M., Pruess, K., 1993. On numerical modeling of capillary barriers. Water Resour. Res. 29 (4), 1045–1056. https://doi.org/10.1029/92WR02875.

Rahardjo, H., Satyanaga, A., Harnas, F.R., Leong, E.C., 2016. Use of dual capillary barrier as cover system for a sanitary landfill in Singapore. Indian Geotec. J. 46 (3), 228–238. https://doi.org/10.1007/s40098-015-0173-3.

Ross, B., 1990. The diversion capacity of capillary barriers. Water Resour. Res. 26 (10), 2625–2629. https://doi.org/10.1029/WR026i010p02625.

Röwer, I.U., Scharff, H., Pfeiffer, E.-M., Gebert, J., 2016a. Optimized landfill biocover for CH4 oxidation I: experimental design and oxidation performance. Current Environm. Eng. 3, 80–93. https://doi.org/10.2174/2212717803666160808123 3.

Röwer, I.U., Streese-Kleeberg, J., Scharff, H., Pfeiffer, E.-M., Gebert, J., 2016b. Optimized landfill biocover for CH4 oxidation II: implications of spatially heterogeneous fluxes for monitoring and emission prediction. Current Environm. Eng. 3, 94–106. https://doi.org/10.2174/2212717803666160804150 3.

Scarfone, R., Wheeler, S.J., Lloret-Cabot, M., 2020. A conceptual hydraulic conductivity model for unsaturated soils at low degree of saturation and application to the study of capillary barrier systems. J. Geotech. Geoenviron. Eng. 146 (10).

Scheutz, C., Kjeldsen, P., Bogner, J., De Visscher, A., Gebert, J., Hilger, H., Huber-Humer, M., Spokas, K., 2009. Microbial methane oxidation processes and technologies for mitigation of landfill gas emissions. Waste Manag. Res. 27 (5), 409–455. https://doi.org/10.1177/0734242X09339325.

Steinert, B. (1999). *Kapillarsperren für die Oberflächenabdichtung von Deponien und Altlasten -Bodenphysikalische Grundlagen und Kipprinnenuntersuchungen-*. [PhD thesis, Universität Hamburg].

Stormont, J.C., 1996. The effectiveness of two capillary barriers on a 10% slope. Geotech. Geol. Eng. 14 (4), 243–267. https://doi.org/10.1007/BF00421943.

Stormont, J.C., Anderson, C.E., 1999. Capillary barrier effect from underlying coarser soil layer. J. Geotech. Geoenviron. Eng. 125 (8), 641–648.

Stormont, J.C., Morris, C.E., 1998. Method to estimate water storage capacity of capillary barriers. J. Geotech. Geoenviron. Eng. 124 (4), 297–302. https://doi.org/10.1061/(asce)1090-0241(1998)124:4(297).

van Dorland, R., Beersma, J., Bessembinder, J., Bloemendaal, N., van den Brink, H., Brotons Blanes, M., Drijfhout, S., Groenland, R., Haarsma, R., Homan, C., Keizer, I., Krikken, F., Le Bars, D., Lenderink, G., van Meijgaard, E., Meirink, J. F., Overbeek, B., Reerink, T., Selten, F., … van der Wiel, K. (2023). *KNMI National Climate Scenarios 2023 for the Netherlands*. Royal Netherlands Meteorological Institute (KNMI). https://cdn.knmi.nl/system/data_center_publications/files/000/071/902/original/KNMI23_climate_scenarios_scientific_report_WR23-02.pdf.

van Genuchten, M.T.; Leij, F.J.; Yates, S.R. (1991). *The RETC Code for Quantifying the Hydraulic Functions of Unsaturated Soils*; Report No. EPA/600/2-91/065. U.S. Environmental Protection Agency, Ada, Oklahoma, United States. https://www.pc-progress.com/Documents/programs/retc.pdfvan.

van Genuchten, M. Th. (1980). A Closed-form Equation for Predicting the Hydraulic Conductivity of Unsaturated Soils. 44(5), 892–898. DOI: 10.2136/sssaj1980.03615995004400050002x.

Van Verseveld, C.J.W., Gebert, J. (2020): Effect of compaction and soil moisture on the effective permeability of sands for use in methane oxidation systems. Waste Managem. 105, 44-53. DOI: 10.1016/j.wasman.2020.03.038.

Ministerie van Volkshuisvesting, Ruimtelijke Ordening en Milieubeheer. (1991). *Richtlijnen voor dichte eindafwerking op afval- en reststofbergingen*. https://www.publicspaceinfo.nl/media/bibliotheek/None/MINVROM%201991%200001.pdf.

Verseveld, C. J. W. (2018). Gas flow through methane oxidation systems: A laboratory and numerical study for optimising. [Master's thesis, Delft University of Technology].

Wang, S., Yang, Y., Luo, Y., Rivera, A., 2013. Spatial and seasonal variations in evapotranspiration over Canada's landmass. Hydrol. Earth Syst. Sci. 17 (9), 3561–3575. https://doi.org/10.5194/HESS-17-3561-2013.

Wawra, B., & Holfelder, T. (2003). Development of a landfill cover with capillary barrier or methane oxidation - the capillary barrier as gas distribution layer. In T. H. Christensen, R. Cossu, & R. Stegmann (Eds.), *Ninth International Waste Management and Landfill Symposium*. CISA, Environmental Sanitary Engineering Centre.

Wolters, D., Homan, C., & Bessembinder, J. (2011). *Ruimtelijke klimatologische verschillen binnen Nederland*. KNMI.

Yang, H., Rahardjo, H., Leong, E.C., Fredlund, D.G., 2004. A study of infiltration on three sand capillary barriers. Can. Geotech. J. 41 (4), 629–643. https://doi.org/10.1139/T04-021.

Yeh, T.-C.-J., Guzman, A., Srivastava, R., Gagnard, P.E., 1994. Numerical Simulation of the Wicking Effect in Liner Systems. Ground Water 32 (1), 2–11. https://doi.org/10.1111/J.1745-6584.1994.TB00604.X.

Zhan, L., Li, G., Jiao, W., Lan, J., Chen, Y., Shi, W., 2020a. Performance of a compacted loess/gravel cover as a capillary barrier and landfill gas emissions controller in Northwest China. Sci. Total Environ. 718, 137195 https://doi.org/10.1016/j.scitotenv.2020.137195.

Zhan, L., Wu, T., Feng, S., Li, G., He, H., Lan, J., Chen, Y., 2020b. Full-scale experimental study of methane emission in a loess-gravel capillary barrier cover under different seasons. Waste Manag. 107, 54–65. https://doi.org/10.1016/J.WASMAN.2020.03.026.

Zhang, A., Bain, J., Schmall, A., Ptacek, C.J., Blowes, D.W., 2024. Seasonal hydrology and gas transport in a composite cover on sulfide tailings. Can. Geotech. J. 61 (5), 854–871. https://doi.org/10.1139/cgj-2022-0606.